

## Supplementary Information

### **Cobalt Modification of Nickel-Iron Hydroxide Electrocatalysts: A Pathway to Enhanced Oxygen Evolution Reaction**

Joshua Zheyang Soo,<sup>1,\*</sup> Asim Riaz,<sup>2,\*</sup> Felipe Kremer,<sup>3</sup> Frank Brink,<sup>3</sup> Chennupati Jagadish,<sup>1,4</sup>  
Hark Hoe Tan,<sup>1,4</sup> Siva Karuturi <sup>2</sup>

<sup>1</sup> Department of Electronic Materials Engineering, Research School of Physics, The Australian National University, 2601 Acton, Australian Capital Territory, Australia

<sup>2</sup> School of Engineering, The Australian National University, 2601 Acton, Australian Capital Territory, Australia

<sup>3</sup> Centre for Advanced Microscopy, The Australian National University, 2601 Acton, Australian Capital Territory, Australia

<sup>4</sup> ARC Centre of Excellence for Transformative Meta-Optical Systems, The Australian National University, 2601 Acton, Australian Capital Territory, Australia

\*Corresponding e-mail: [joshua.soo@anu.edu.au](mailto:joshua.soo@anu.edu.au); [asim.riaz@anu.edu.au](mailto:asim.riaz@anu.edu.au)

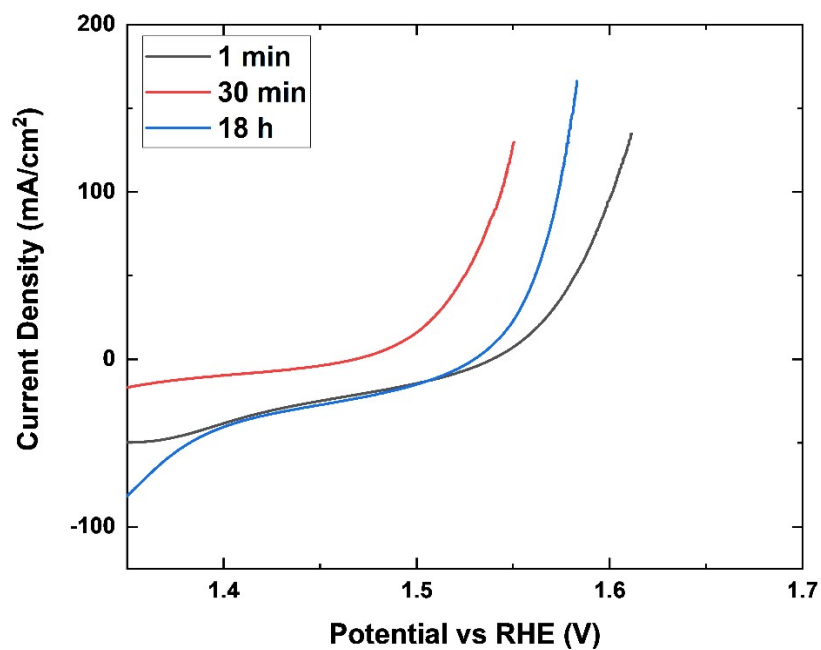


Figure S1: Reverse-scanned LSVs of NiFeCo hydroxide synthesized using 15 mM Co chloride concentration at different corrosion times.

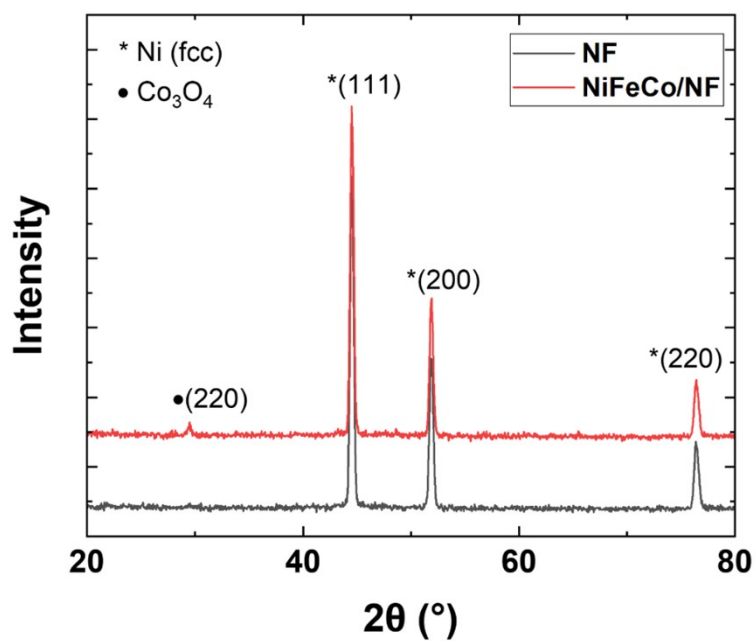


Figure S2: XRD plots of NiFeCo/NF and NF.

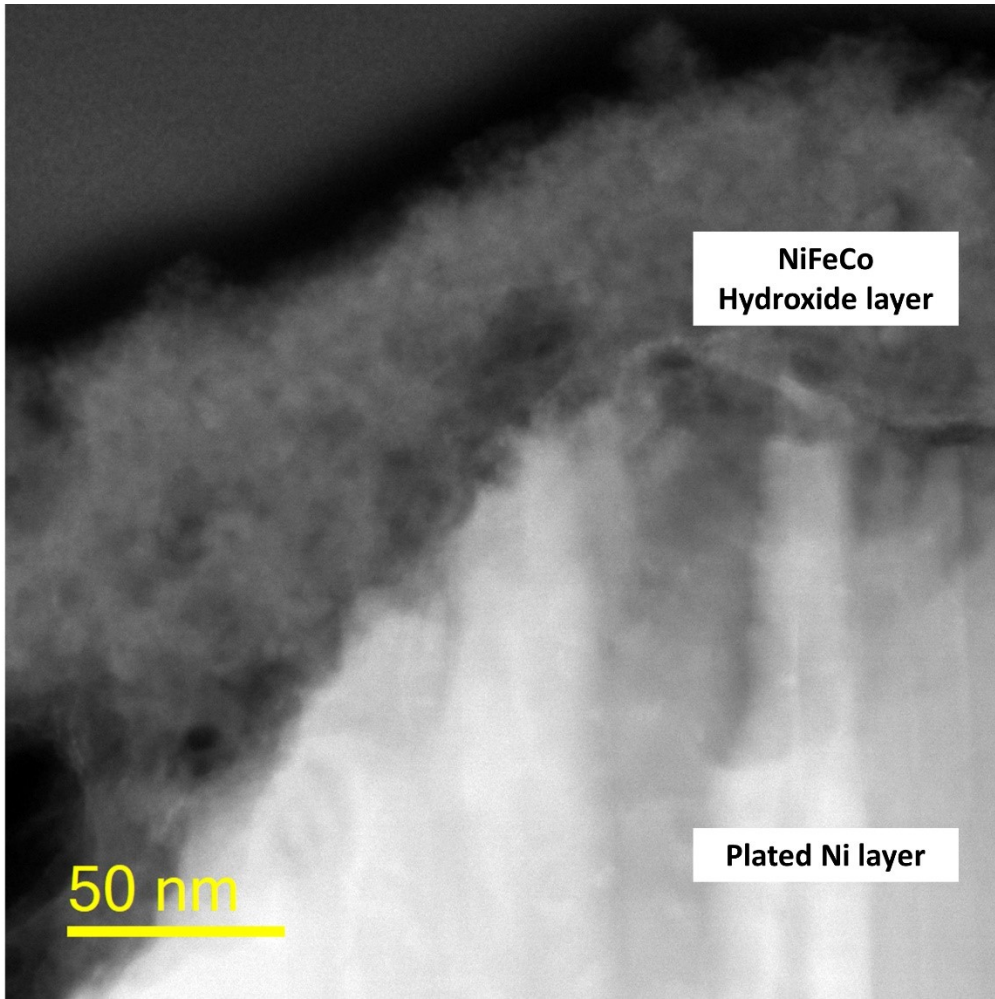


Figure S3: Grayscale of HAADF image of NiFeCo/Si with labelled regions.

**Table S1: Peak assignments of NiFeCo/NF XPS Spectra from Figure 2(d-g).**

Ni 2p			Fe 2p		
Peak	Energy (eV)	Assignment	Peak	Energy (eV)	Assignment
1	852.8	Ni <sup>0</sup> 2p <sub>3/2</sub>	1	710.6	Fe <sup>3+</sup> 2p <sub>3/2</sub>
2	855.6	Ni <sup>2+</sup> 2p <sub>3/2</sub>	2	712.5	Fe <sup>3+</sup> 2p <sub>3/2</sub> , (multiplet)
3	857.2	Ni <sup>3+</sup> 2p <sub>3/2</sub>			
4	861.1	Ni <sup>2+</sup> 2p <sub>3/2</sub> , sat			
5	863.7	Ni <sup>3+</sup> 2p <sub>3/2</sub> , sat			

Co 2p			O 1s		
Peak	Energy (eV)	Assignment	Peak	Energy (eV)	Assignment
1	781.0	Co <sup>2+</sup> 2p <sub>3/2</sub>	1	529.9	M-O bonds
2	782.4	Co <sup>3+</sup> 2p <sub>3/2</sub>	2	531.6	M-OH bonds
3	786.8	Co <sup>2+</sup> 2p <sub>3/2</sub> , sat	3	532.9	Adsorbates
4	789.8	Co <sup>3+</sup> 2p <sub>3/2</sub>			

**Table S2: Comparison of NiFeCo/NF with other NiFeCo electrocatalysts and Ni-based electrocatalysts synthesized using solution corrosion method.**

Sample	Synthesis Method	OER overpotential at	Ref
--------	------------------	----------------------	-----

<b>10 mA/cm<sup>2</sup> (mV)</b>			
<b>NiFeCo/NF</b>	<b>Solution corrosion</b>	<b>195</b>	<b>Own work</b>
NiFeCo/Iron foil	Hydrothermal	300	1
NiFeCo/NF	CV electrodeposition	207	2
NiFeCo/Ti felt	Co-precipitation	249	3
NiFeOOH/NiFeS <sub>x</sub> /NiFe foam	Solution corrosion	227	4
NiFe LDH/NF	Solution corrosion	180	5
NiFe LDH/NF	Solution corrosion	269	6

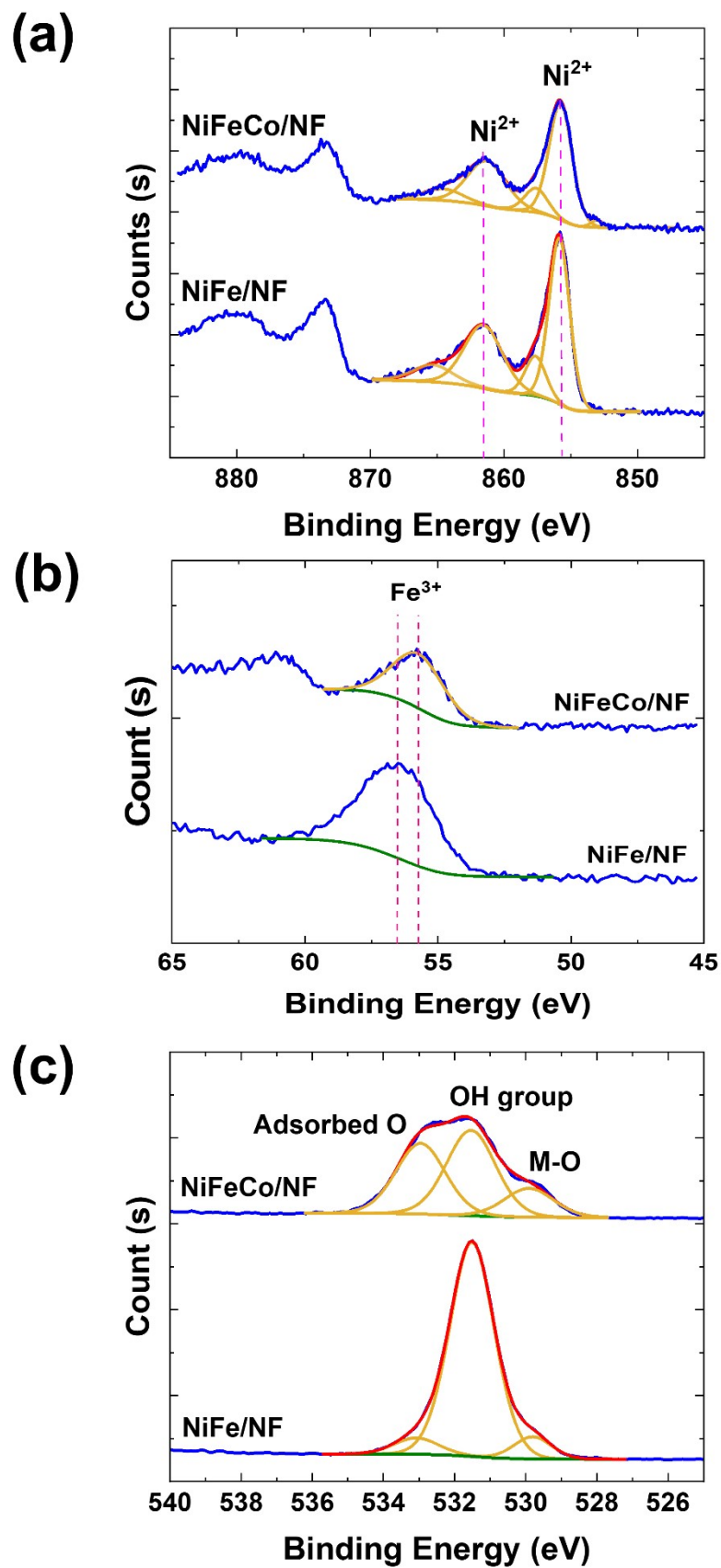


Figure S4: (a) Ni 2p, (b) Fe 3p, and (c) O 1s XPS spectra of NiFe/Si and NiFeCo/Si

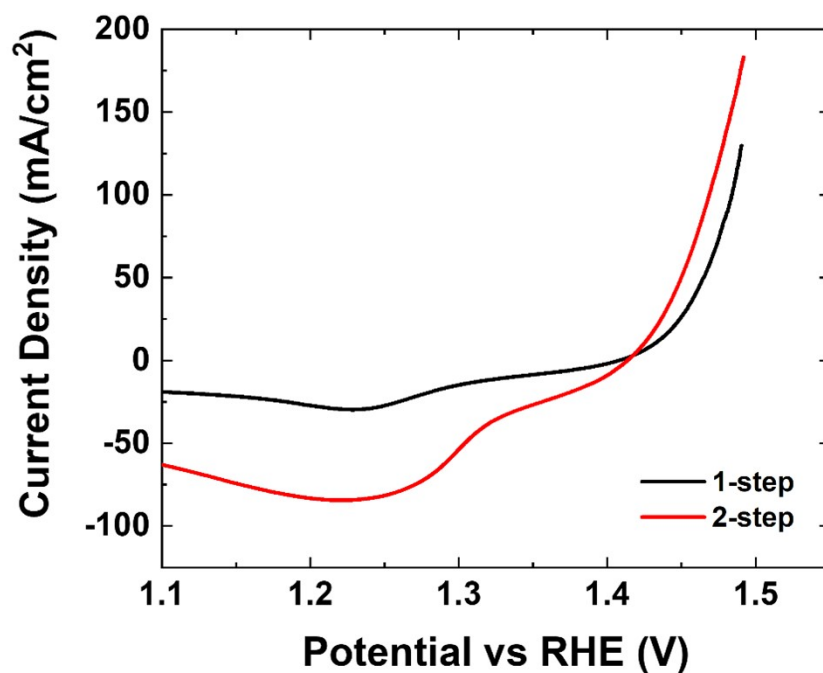


Figure S5: LSVs of NiFeCo/NF synthesized using 1 or 2-step processes.

Table S3: Randles cell equivalent circuit values of NiFe/Si and NiFeCo/Si

Sample	$R_s$	$R_{ct}$	CPE ( $Y_0$ )	CPE (N)
NiFe/Si	0.965	0.590	0.028	0.651
NiFeCo/Si	0.812	0.269	0.092	0.789

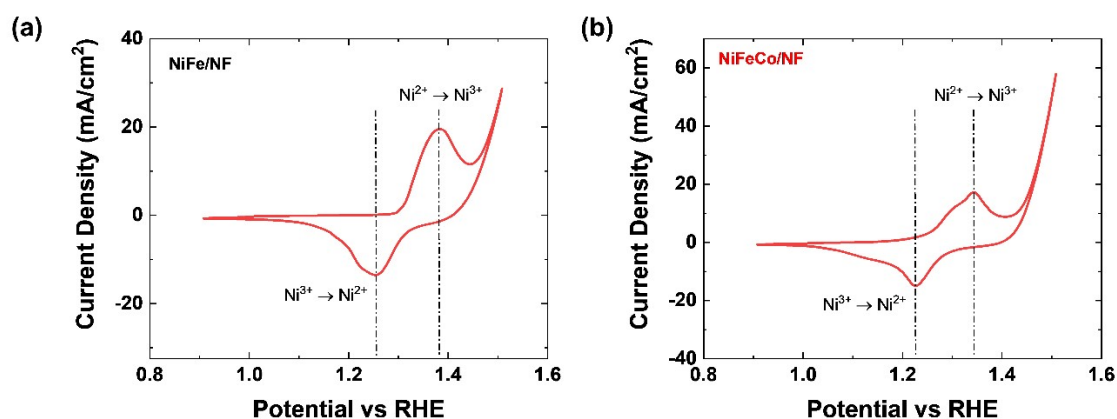


Figure S6: CV of (a) NiFe/NF and (b) NiFeCo/NF with labelled  $Ni^{2+}$ - $Ni^{3+}$  redox couple.

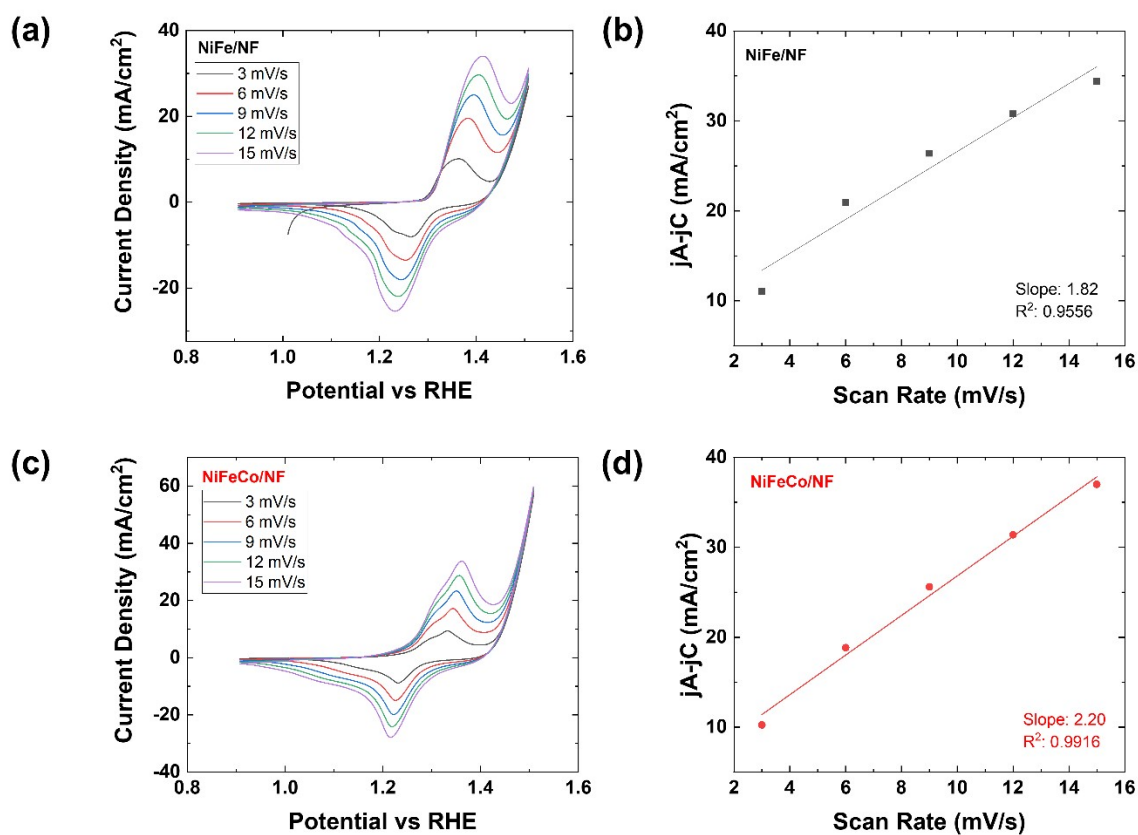


Figure S7: CV graphs at various scan rates (3 – 15 mV/s) and corresponding linear fitted plots of the maximum difference of anodic and cathodic sweep current densities vs scan rate for: (a-b) NiFe/NF and (c-d) NiFeCo/NF.



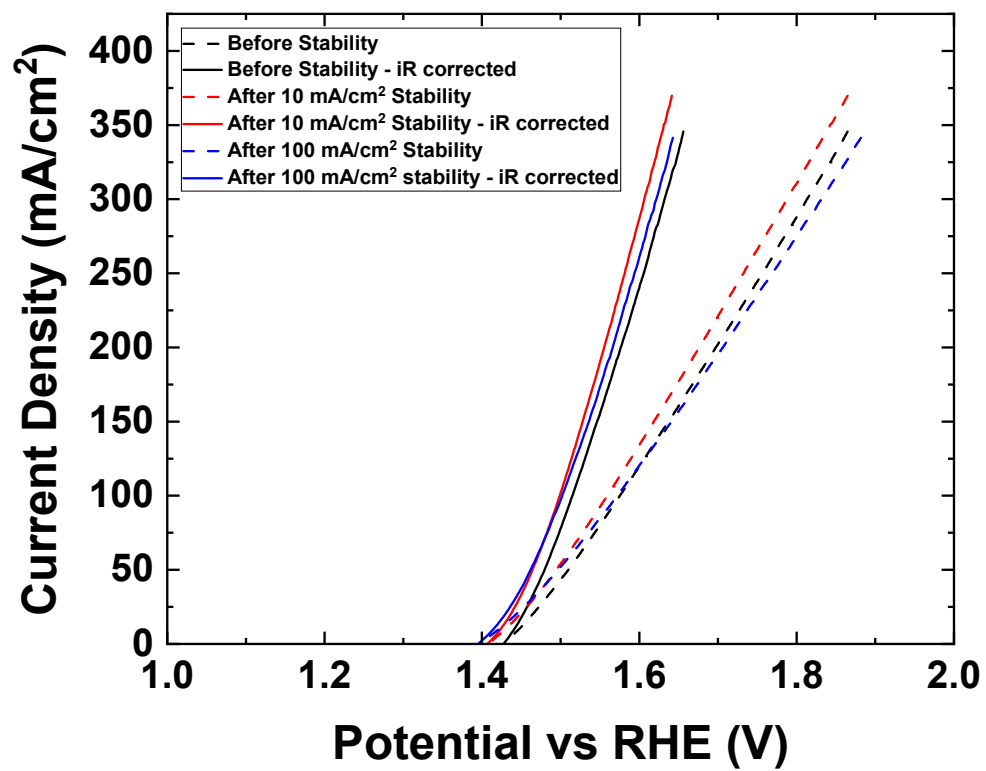


Figure S8: LSVs of NiFeCo/NF before and after chronopotentiometry (stability).

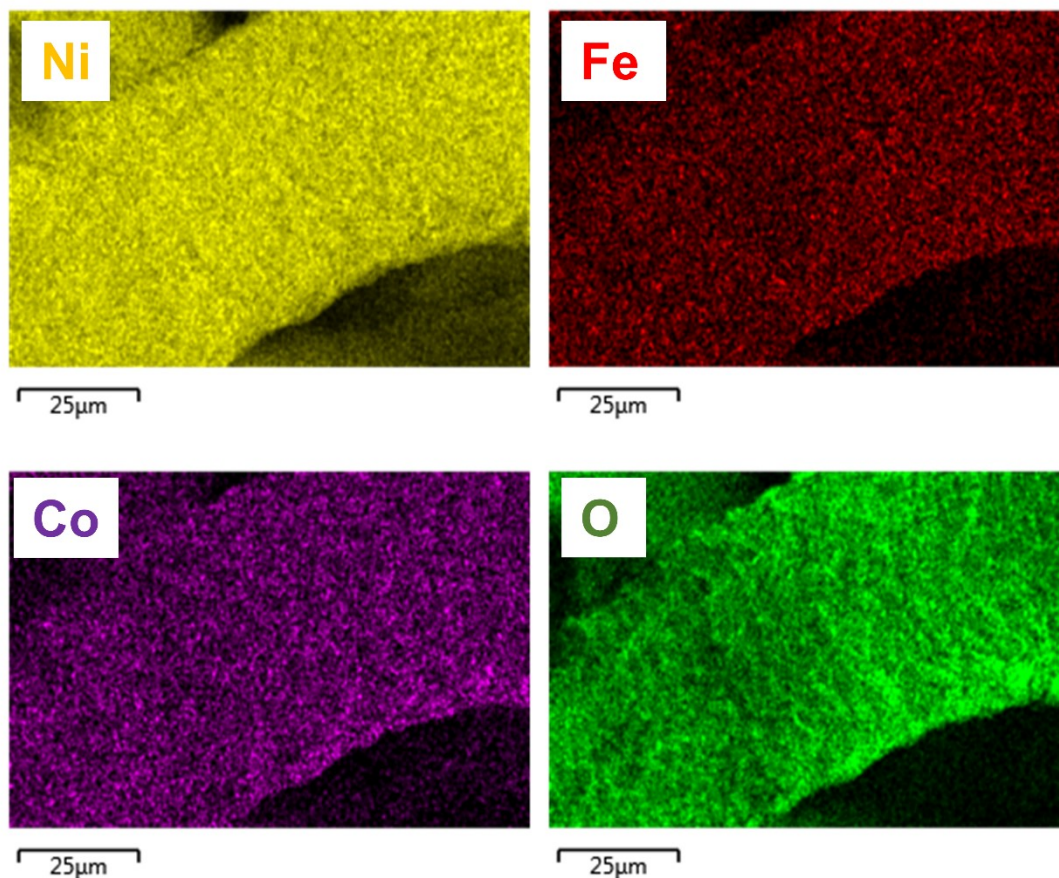


Figure S9: EDX of NiFeCo/NF surface after chronopotentiometric measurements.

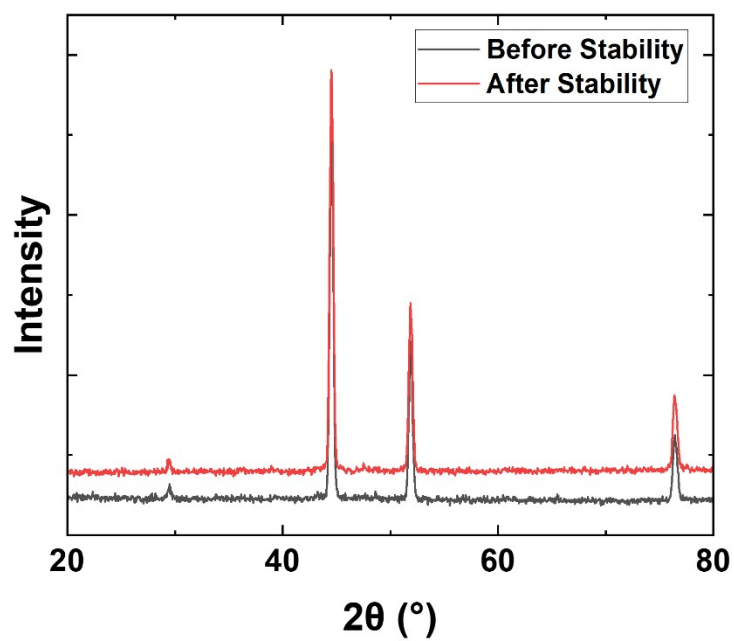


Figure S10: XRD plots of NiFeCo/NF before and after chronopotentiometry (stability) measurements.

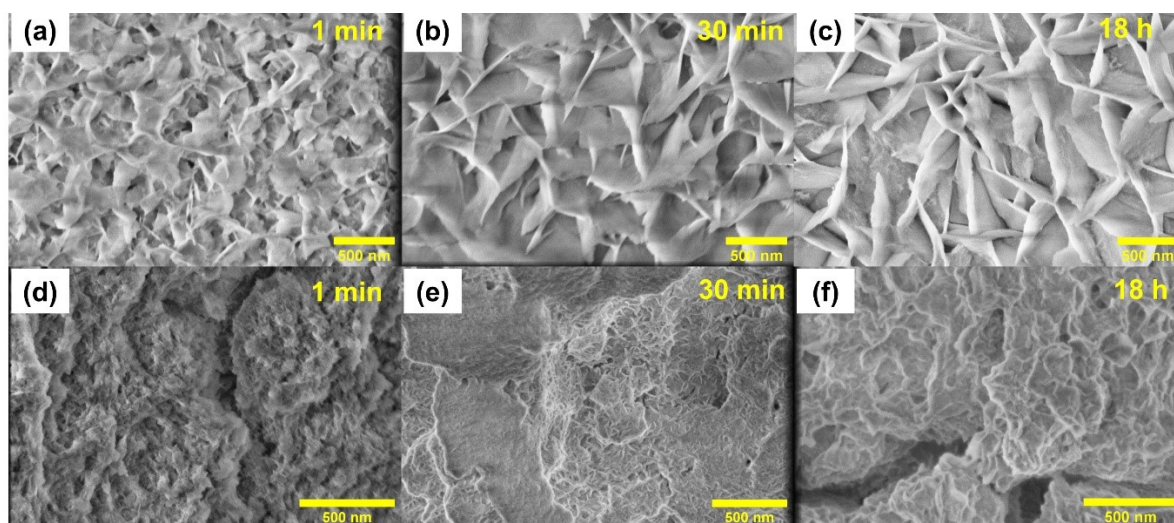


Figure S11: SEM images of NiFeCo synthesized using (a-c): Co chloride precursor and (d-f) Co nitrate precursor at different synthesis times.

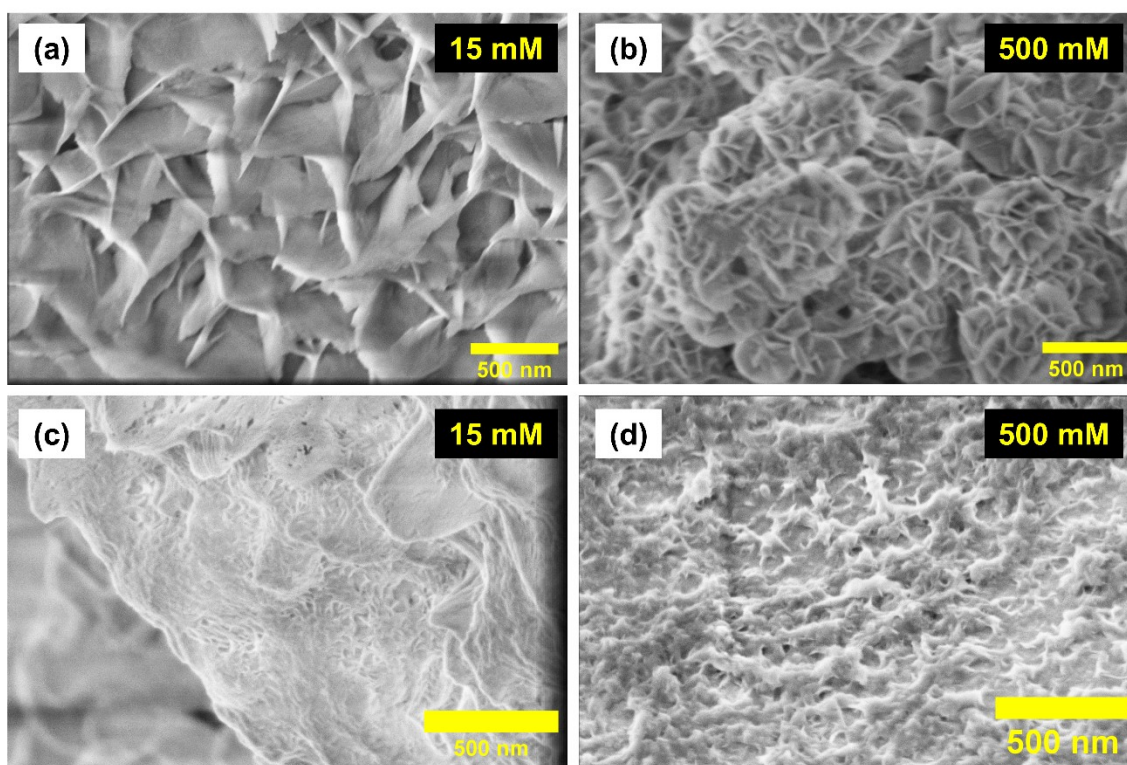


Figure S12: SEM images of NiFeCo/NF synthesized with (a-b) Co chloride precursor and (c-d) Co nitrate precursor; synthesized at 15 mM and 500 mM precursor concentrations, respectively.

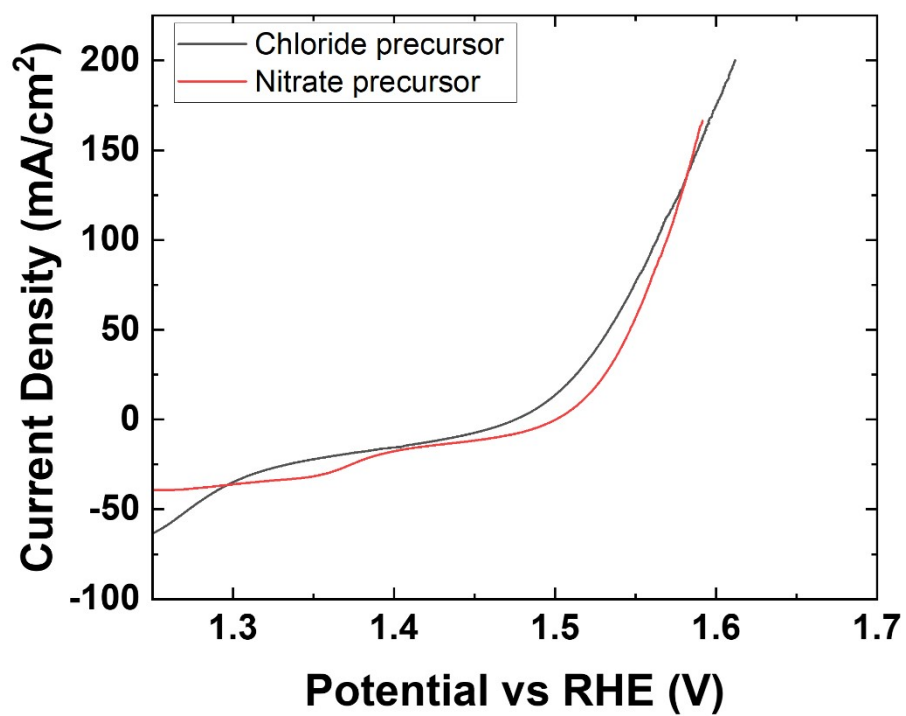


Figure S13: LSVs of NiFeCo/NF synthesized using different Co precursors at 15 mM concentration.

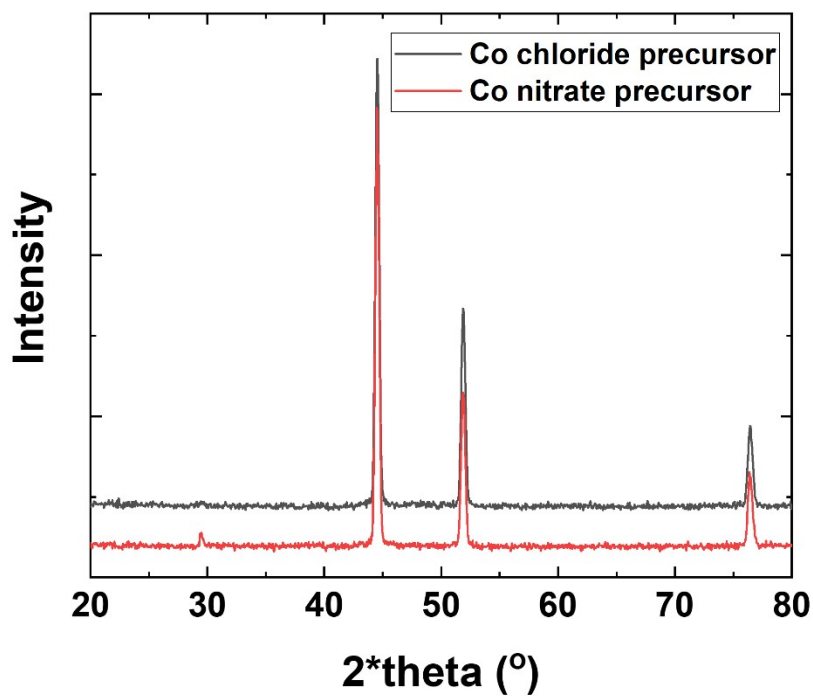


Figure S14: XRD plots of NiFeCo/NF synthesized using Co chloride and Co nitrate precursors at 15 mM precursor concentration.

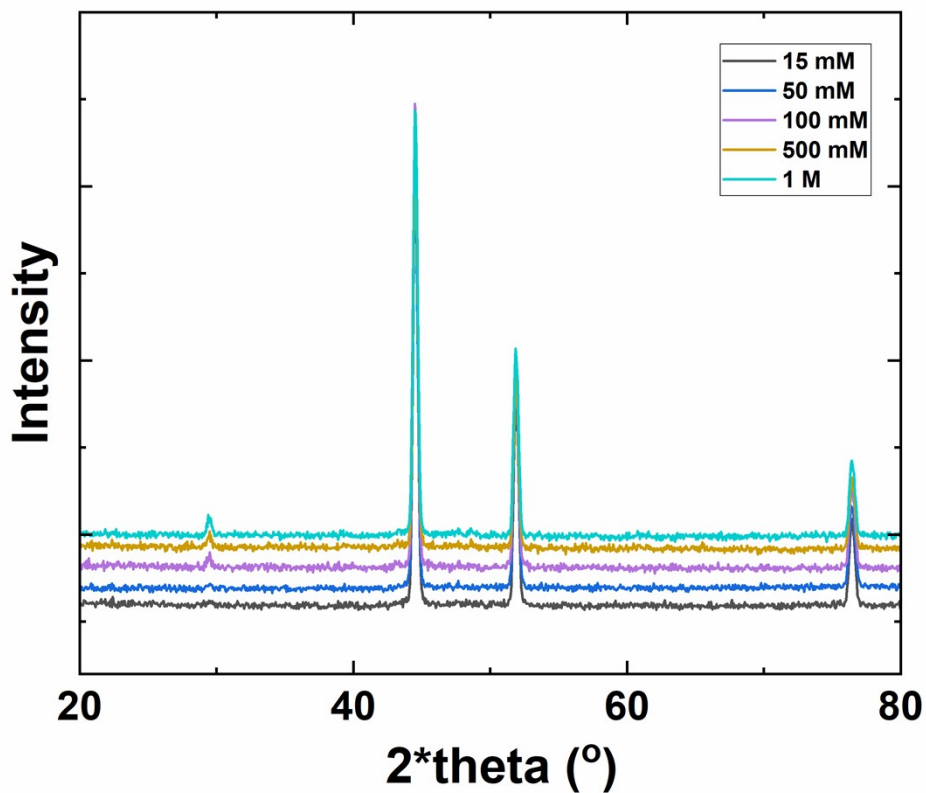


Figure S15: XRD plots of Co-chloride synthesized NiFeCo/NF at different precursor concentrations.

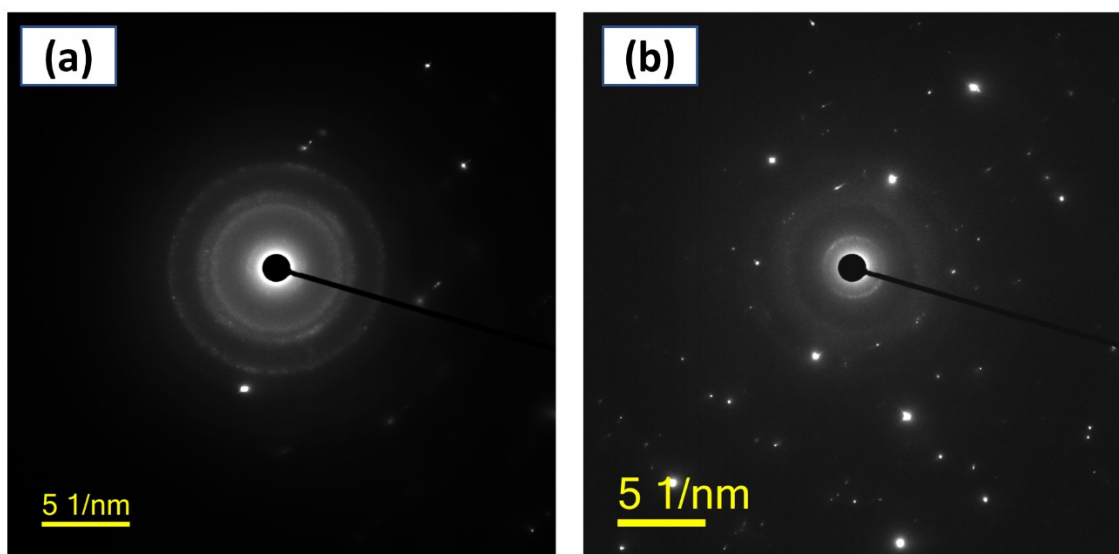


Figure S16: SAED patterns of Co -chloride synthesized NiFeCo/Si synthesized at (a) 15 mM and (b) 1 M precursor concentrations.

Table S4: pH values of Co chloride solution at different concentrations.

Co chloride concentration (mM)	Solution pH
15	7.0
50	7.0
100	6.7
500	6.2
1000	5.7

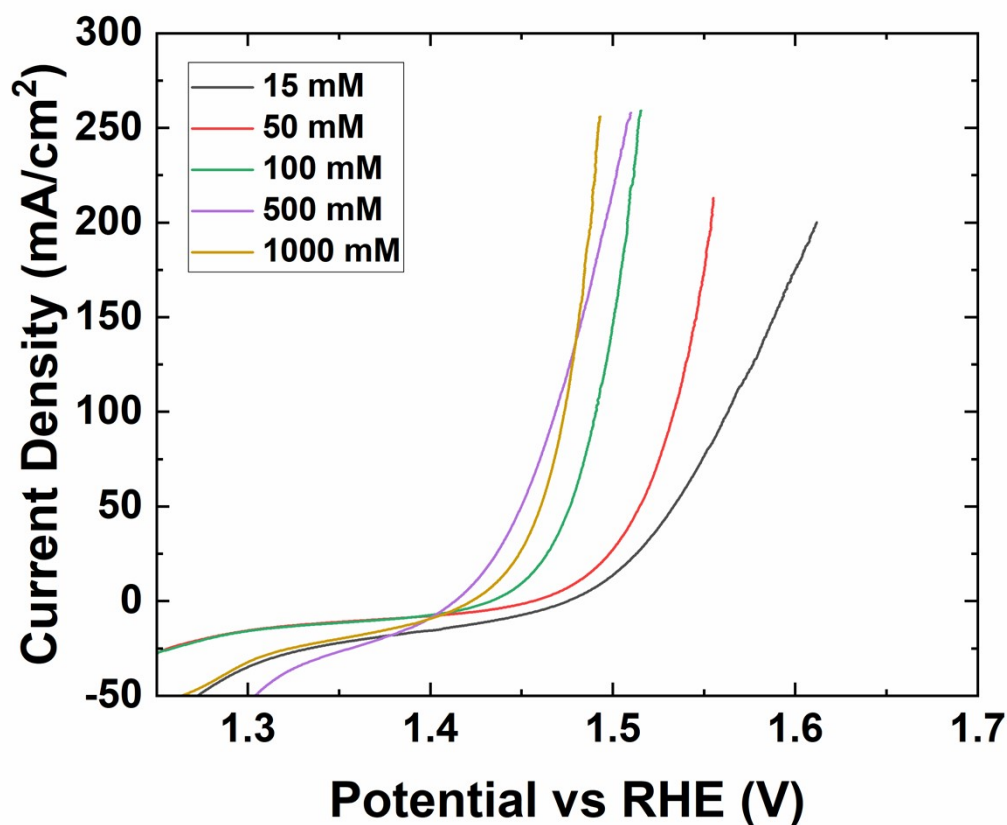


Figure S17: Reverse-scanned LSV of Co-chloride synthesized NiFeCo/NF at different Co chloride concentrations.

Table S5: Estimated  $R_{ct}$  values of Co-chloride synthesized NiFeCo/NF obtained from Nyquist plots in Figure 4(d).

Precursor Concentration (mM)	$R_{ct}$ of NiFeCo/NF ( $\Omega$ )
15	1.010
50	0.677
100	0.570
500	0.520
1000 (1 M)	0.676

## References:

1. M. L. Lindstrom, R. Gakhar, K. Raja and D. Chidambaram, *Journal of The Electrochemical Society*, 2020, **167**, 046507.
2. H. Y. Jung, J. H. Park, J. C. Ro and S. J. Suh, *ACS Omega*, 2022, **7**, 45636-45641.
3. Y. S. Park, J.-Y. Jeong, M. J. Jang, C.-Y. Kwon, G. H. Kim, J. Jeong, J.-h. Lee, J. Lee and S. M. Choi, *Journal of Energy Chemistry*, 2022, **75**, 127-134.
4. M. Chen, W. Li, Y. Lu, P. Qi, H. Wu, G. Liu, Y. Zhao and Y. Tang, *Journal of Materials Chemistry A*, 2023, **11**, 4608-4618.
5. Y.-F. Song, Z.-Y. Zhang, H. Tian, L. Bian, Y. Bai and Z.-L. Wang, *Chemistry – A European Journal*, 2023, **29**, e202301124.
6. Y. Liu, X. Liang, L. Gu, Y. Zhang, G.-D. Li, X. Zou and J.-S. Chen, *Nature Communications*, 2018, **9**, 2609.